Journal of Cellular Biochemistry 22:15–29 (1983)
Biosynthesis of the Photosynthetic Apparatus:
Molecular Biology, Development and Regulation 15–29

Biosynthesis of the Photosynthetic Membranes of Rhodopseudomonas sphaeroides

Samuel Kaplan, Brian D. Cain, Timothy J. Donohue, William D. Shepherd, and Grace S. L. Yen

Department of Microbiology, University of Illinois, Urbana, Illinois 61801

The steady-state biosynthesis of the photosynthetic membrane (ICM) of Rhodopseudomonas sphaeroides has been reviewed. At moderate light intensities, 500 ft-c, preexisting ICM serves as the insertion matrix for newly synthesized membrane components. Whereas the bulk of the membrane protein, protein-pigment complexes, and pigments are inserted into preexisting ICM throughout the cell cycle, phospholipid is transferred from outside the ICM to the ICM only at the time of cell division. Because the site of cellular phospholipid synthesis is the cytoplasmic membrane, these results infer that despite the physical continuity of cytoplasmic membrane and ICM, there must exist between these membranous domains a "barrier" to the free diffusion of cellular phospholipid. The cyclical alternation in protein to phospholipid ratio of the ICM infers major structural and functional alternations, such as changes in the protein to lipid ratio of the membrane, specific density of the membrane, lipid structure within the membrane, and the rate of cyclic electron flow. When biochemical studies are correlated with detailed electron microscopic investigations we can further conclude that the number of photosynthetic units within the plane of the membrane can vary by nearly a factor of two over the course of the cell cycle. The average physical size of the photosynthetic units is constant for a given light intensity but inversely proportional to light intensity. The distribution of photosynthetic unit size classes within the membrane can be interpreted as suggesting that the "core" of the photosynthetic unit (reaction center plus fixed antenna complex) is inserted into the membrane coordinately as a structural entity. The variable antenna complex is, on the other hand, inserted independent of the "core" and randomly associates with both old and new core complexes. Finally, we conclude that there is substantial substructure to the distribution of photosynthetic units within the ICM, ie, they are highly ordered and exist in a defined spatial orientation to one another.

Received May 5, 1983; revised and accepted July 13, 1983

monas sphaeroides growing under moderate but saturating light intensity. Further, an effort has been made to correlate studies which are currently underway to those which have been published in recent years.

In previous studies from our laboratory [1–4] employing steady-state, synchronous cultures of R sphaeroides we have shown that preexisting ICM serves as the matrix for the accumulation of new ICM-specific protein during the cell cycle. All of the major ICM proteins, in particular the bacteriochlorophyll-(Bchl)-binding proteins, are accumulated in constant proportions and at constant rates, relative one to another. Similarly, photopigments, both carotenoids and Bchl, are inserted into preexisting ICM throughout the division cycle. However, unlike protein, ICM phospholipid is not accumulated into preexisting ICM until the time of cell division, when previously synthesized [5] phospholipid is transferred from outside the ICM to the ICM. Because phospholipid accumulated throughout the division cycle and residing most probably within the cytoplasmic membrane (CM) does not equilibrate with ICM phospholipid, we postulate the existence of a "barrier" [5] between these continuous membrane systems [6,7]; one which prevents the free, lateral movement of phospholipid. As a result of this temporal dissociation between protein and phospholipid accumulation into the ICM, the ratio of protein to phospholipid within the ICM oscillates in a cell-cycle specific manner between a low of approximately 2.4:1 just following cell division and a high of approximately 5.0:1 just prior to cell division [4].

Pictorially, these data have been represented in Figure 1. Let us view an invagination as consisting of a phospholipid bilayer in which are embedded photosynthetic units whose size is dependent upon the incident light intensity. Large multimeric aggregates composed of reaction centers (RC) and fixed antennae pigment-proteins, B875-complex (LHI) comprise the fixed photosynthetic unit (FPU). In turn, these FPUs are surrounded by the variable antenna B800-850 (LHII) complexes and together with the FPU comprise the variable photosynthetic unit (VPU). Coupling factor protrudes towards the interior of the cell. Following cell division, the packing density of the variable photosynthetic units (VPU) within the bilayer is reasoned to be low. As we proceed through the division cycle, at constant light intensity, the composition and presumably size of the VPU remains constant but the packing density is thought to increase until a point, just prior to cell division, at which time the packing density of VPUs would reach its maximum.

Our results and their interpretations have important implications for structure, function, regulation of assembly, and partitioning of ICM to daughter cells at cell division. If we first consider the structure, within the bilayer, of ICM phospholipids during the division cycle as measured by the fluorescence polarization of the probe α-parinaric acid [8], we observe that as the protein to phospholipid ratio increases the fluorescence polarization increases and then decreases as the protein to phospholipid ratio decreases [9]. If we plot the microviscosity of the membrane versus the percent by weight of ICM protein in Figure 2 we observe a dramatic change in the inferred structure of ICM phospholipid where we would predict that the bulk of the ICM phospholipid may become immobilized due to its association with protein. The magnitude of these changes is the equivalent of those which may be produced by a greater than 15°C change in temperature. Expressed another way, the structure of the ICM during the cell cycle can be envisioned to fluctuate between approximately 8 phospholipid molecules per polypeptide of 27,000 molecular weight to 4 phospho-

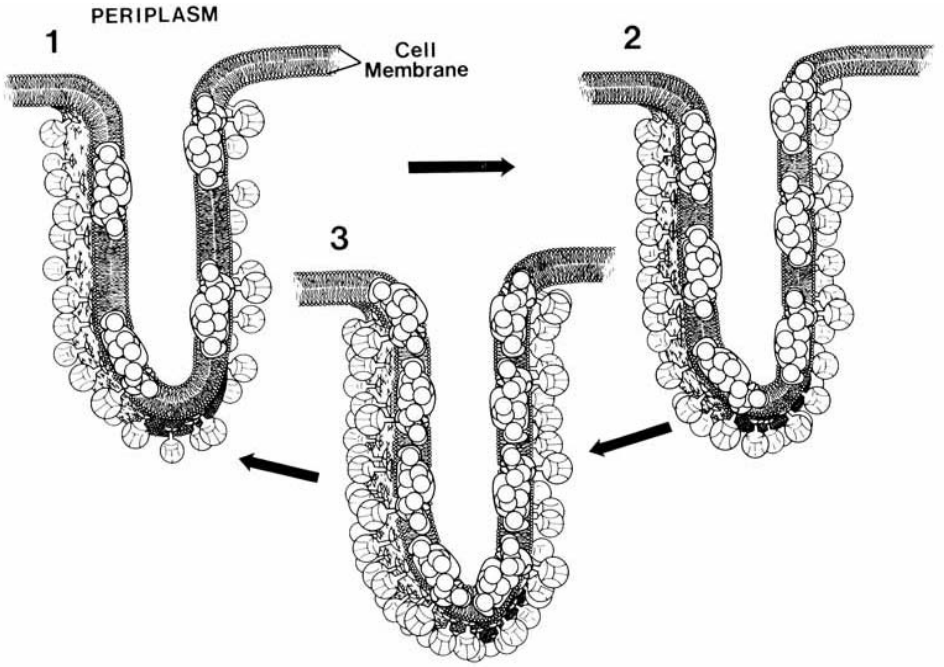

Fig. 1. Illustration of a preexisting intracytoplasmic membrane invagination depicting its replication just following cell division (1), midway through the cell cycle (2), and just prior to cell division (3). The large multimeric aggregates within the membrane are photosynthetic units. The F_1 portion of the ATPase protrudes into the cytoplasm.

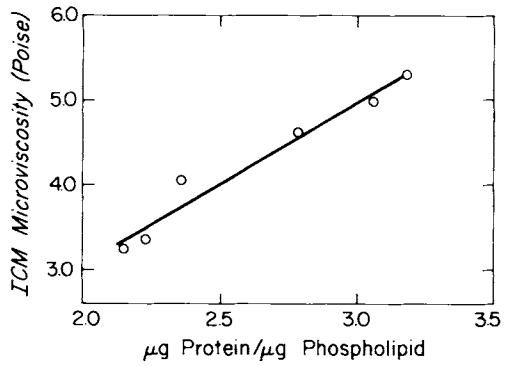

Fig. 2. Microviscosity of chromatophores isolated from cells at various points in the cell cycle versus the protein to phospholipid weight ratio of the chromatophores.

lipids per polypeptide of 27,000 molecular weight [10]. This same effect can be observed by following the intrinsic density of the chromatophores as we proceed through the division cycle [4].

Another implication of these results bears significantly on the structure and distribution of VPU within the ICM as the cells proceed through the division cycle.

Drews and colleagues [11] and others [12,13] have demonstrated that the size of the intramembranous particles observed from freeze-fracture preparations are compatible with their being multimeric aggregates of RC with both fixed B875 antenna complexes and B800-850 antenna. Therefore, we would predict that in steady-state cells the size of the freeze fracture particles, VPUs, should remain constant but the distance between particles should change, ie, more particles should be inserted, as we proceed through the division cycle. Because of the very small size, 50–60 nm and high radius of curvature of isolated ICM vesicles, (chromatophores), it is difficult if not impossible from freeze-fracture studies of isolated vesicles to obtain the kind of quantitative data detailing particle size and number. Likewise, because of the vesicular nature of the ICM of R sphaeroides similar studies on intact cells are also very difficult. Therefore, we set about to improve the utility of our experimental material by enlarging the size of isolated chromatophores. This was achieved by fusing isolated chromatophores using polyethylene glycol and Ca^{2+}. In a study, recently published [14], we have demonstrated that these "fused" vesicles are structurally identical to untreated chromatophores. As a result of chromatophore fusion, vesicle size was appreciably increased and the resulting vesicles proved to be excellent material for freeze-fracture analysis, as shown in Figure 3a. Whereas, isolated chromatophores are extremely difficult to employ in freeze-fracture studies to derive quantitative data as to particle size and density, the fused products are amenable to such an analysis.

RESULTS

To analyze the size and particle distribution of VPUs, steady-state photoheterotrophic cultures of R sphaeroides were grown under synchronous culture conditions [1–3], and cells were harvested at various times along the cell cycle. Chromatophores were purified employing standard conditions developed in our laboratory [15]. Purified chromatophores were shown to have unique protein to phospholipid ratios depending upon the point in the cell cycle from which the sample was obtained [4]. Chromatophores from each sample were then fused employing published procedures [14]. As a result we were able to obtain large vesicles for each sample of chromatophores which were in turn used in our freeze-fracture studies. Please note, we did not fuse chromatophores between samples only within samples. We then proceeded to measure particle number, particle size, interparticle distance and particle distribution. All the values presented are at the 98–99% confidence limits.

In Figure 4 (see also Table 1) we have plotted the number of particles per 10^4 nm^2 versus the protein to phospholipid ratio of the input, purified chromatophores. The circles represent six samples derived from several independent and sequential synchronous cultures. As you can see there is a linear relationship between the particle density and the ratio of protein to phospholipid. The sample designated by the square is derived from an asynchronous culture grown at the same light intensity and as would be expected, this value also falls nicely on the curve. When samples from other synchronous cell experiments, not shown here, are similarly analyzed, providing they are grown at the same light intensity, they fall nicely onto this straight line. It is important to point out why several independent cell synchronies were performed in order to generate the material for analysis: 1) The volume of sample required was substantial and could not be conveniently scaled-up beyond 4.6 liters. 2) When dealing with synchronous cultures it was not obvious as to precisely where

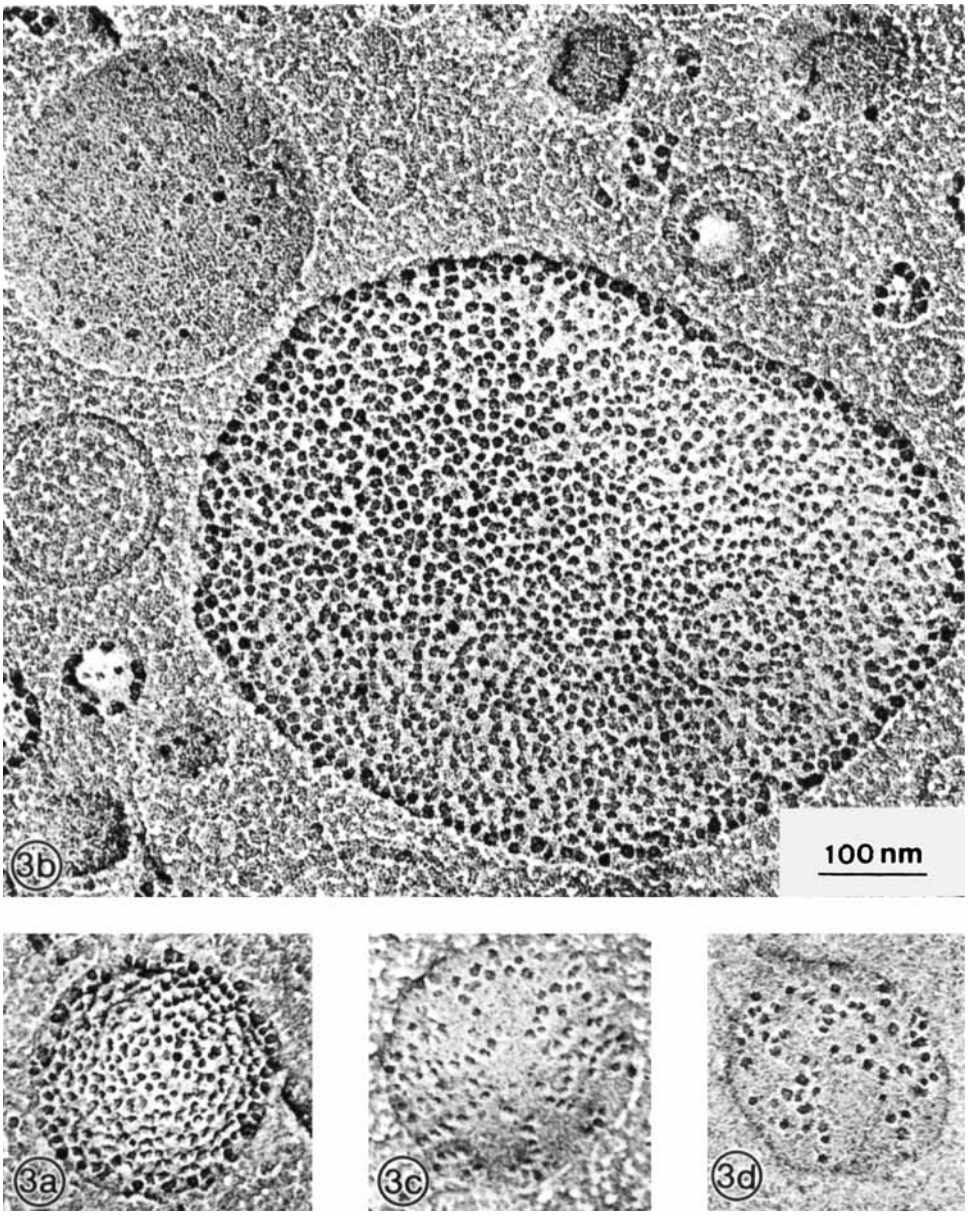

Fig. 3. High magnification electron micrographs of freeze-fracture replicas of fused chromatophores and chromatophore-liposome fusion products. Fusion substrates were incubated in the presence of 55% polyethylene glycol (PEG) 6000 (final concentration, w/v) at 33°C for 1 hr. For chromatophore-liposome fusion, liposomes were added to purified chromatophores at three different phospholipid weight ratios, 1:1, 1:5, and 1:10 (chromatophore phospholipid:liposome phospholipid). Each fusion mixture was layered on a discontinuous sucrose gradient (8, 16, 24, 40% sucrose in 10 mM NaH_2PO_4, w/v, pH 7.0) and centrifuged in a Beckman SW28 rotor at 100,000g for 14 hr at 4°C. Distinct membrane fractions of different density distributions were collected. a) Fused chromatophores, protein/phospholipid ratio 3.7; b–d) chromatophore-liposome fusion products with protein/phospholipid ratio of 3.18 1.55, and 1.14, respectively. Bar represents 100 nm × 150,000.

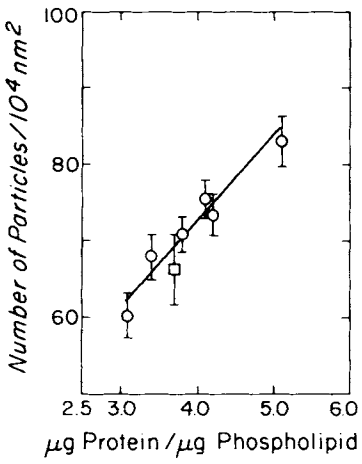

Fig. 4. Effect of chromatophore protein/phospholipid ratio on the intermembrane particle density of the PF face of fused chromatophores. For intramembrane particle density determinations, all negatives were taken at 50,000× and optically enlarged to 500,000×. A 33.4-mm test circle (corresponds to object area of 3500 mm^2) was applied to the center of an enlarged fracture face. At least 50 fracture faces were analyzed and 1035 to 1500 particles counted for each sample. The raw data were then converted to number of particles/10^4 nm^2 and plotted against protein/phospholipid ratio. Circles, purified chromatophores isolated from six culture samples from three different synchrony experiments. Square, purified chromatophores isolated from asynchronous culture of R sphaeroides grown under similar culture conditions at 500 ft-c. Bars represent 99% confidence limits.

TABLE I. A Summary of Particle Distribution, Numbers, and Size in Freeze-fracture Preparations of Fused Chromatophores

Sample	Protein/ phospholipid	Number of particles/ 10^4 nm^2	Mean particle size (nm)	% Area covered by particles	Particle distance (nm) center to center	Particle distance (nm) edge to edge
4000 ft-c	2.83	68.3	8.25	36.5	13.77	5.52
500 ft-c	3.70	66.3	9.08	42.9	14.00	4.92
30 ft-c	3.43	74.8	9.75	55.8	13.07	3.32
Synchrony samples #1	3.1	60.3	9.10	39.2	14.78	5.68
#2	3.4	67.9	9.11	44.3	13.81	4.70
#3	3.8	70.8	9.04	45.4	13.49	4.45
#4	4.2	73.4	9.05	47.2	13.21	4.16
#5	4.1	75.4	9.13	49.4	13.02	3.89
#6	5.1	82.9	9.02	53.0	12.34	3.32
Chromatophore/ liposome fusion gradient fraction						
B-I	1.14	26.3	9.25	17.7	24.22	14.97
C-II	1.36	40.8	9.08	26.4	18.56	9.48
A-II	3.18	70.7	9.33	48.3	13.50	4.17

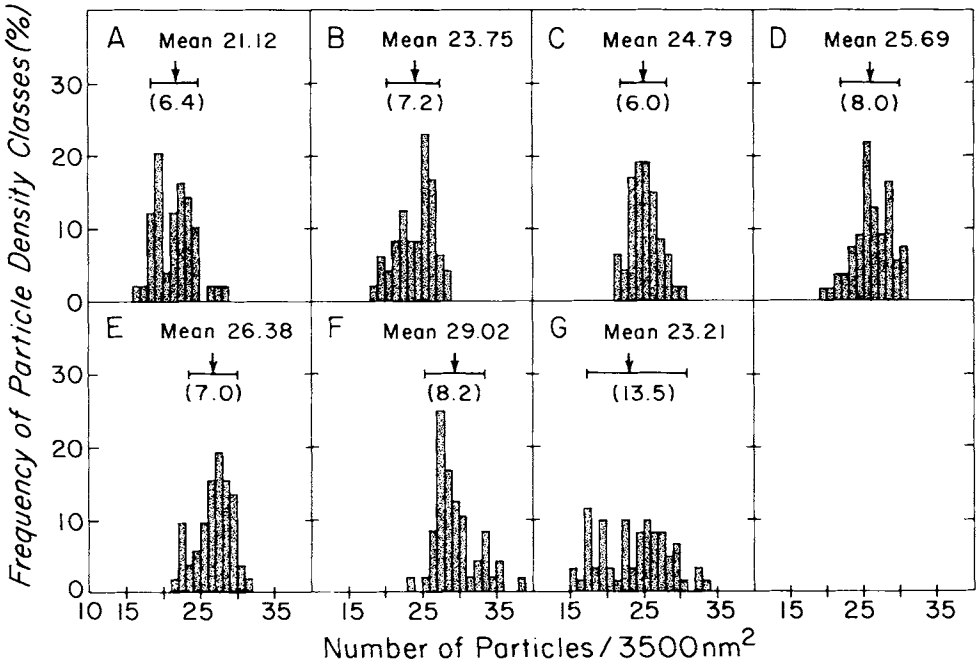

Fig. 5. PF-face particle density histograms of fused chromatophores isolated from synchronous (A–F) and asynchronous (G) cultures grown photoheterotrophically. Arrows indicate the mean particle density for each sample. Horizontal bar and the number in parenthesis show the distribution range of 83.3%, centered at the mean, of the sample population measured. The protein/phospholipid ratios of samples in A–G are 3.1, 3.4, 3.8, 4.2, 4.1, 5.1, and 3.7, respectively.

within the cell cycle the sample was derived until the experiment was terminated. Once a series of synchronies were performed samples were selected for analysis only on the basis that they represented cells at different points in the cell cycle. Normally, such an approach might be expected to compromise the quality of the data obtained; however, the data in Figure 4 show that this is clearly not the case.

In Figure 5, we have plotted a histogram of the frequency of particle density classes versus the number of particles per 3500 nm^2. The important points to note here are the following. For the samples derived from the synchronous cultures (panels A–F) the distributions are relatively narrow and the 2 ς error bar about each sample is relatively constant. Remember, that even in a good synchronous culture, easily 15–25% of the cells are not in synchrony. However, in panel G, the asynchronous sample shows a very broad distribution of particle density classes and the 2 ς error bar is roughly twice that for the average of the samples derived from synchronous cells. This result vividly explains the polydisperisity of replicating chromatophore samples initially demonstrated by Kosakowski and Kaplan [16], which led our laboratory to question the mode replication of the ICM in steady-state cultures of R sphaeroides. It is also important to note from this figure that both the lower and upper extremes in particle density classes increase as we proceed through the cell cycle. By comparison the sample from an asynchronous culture shows a broad flat distribution but encompasses the same extremes.

Further, if we examine the particle diameter of samples obtained either from a synchronous or an asynchronous culture grown under moderate but saturating light intensity (see Table I), we observe that the size distribution is narrow and constant at a mean value of 9.08 $\pm$ 0.12 nm. Further, we can calculate that during the course of the cell cycle, of the total bilayer area, as little as 33% and as much as 60% can be occupied by 9.08-nm particles, which we believe represent the VPU.

When we compare particle density and particle size derived from samples obtained from asynchronous cultures grown at high (4000 ft-c), medium (500 ft-c), and low (30 ft-c) light intensities (Fig. 6) we observe: 1) The particle density of high and medium light grown cells to be the same while that of low light cells is approximately 10% higher and 2) the average particle diameter to increase from 8.25 nm for high light grown cells, to 9.08 nm for medium light grown cells to 9.75 nm for low light grown cells at 99% confidence limits (see also Table I). The fact that the particle size varies inversely to light intensity is in concert with the prediction that these particles contain reaction center and both fixed and variable antenna components. The fact that the high light-grown cells show a considerably narrower distribution of particle sizes than that seen in cells grown at low light intensities suggests that the variable pigment-protein complex, B800-850, may distribute randomly on the fixed photosynthetic unit, core. Since lower light intensity gives rise to greater cellular levels of B800-850 complexes, the particle size distribution in low light grown cells might be expected to show greater dispersity than that found in high light grown cells if LHII associations occur at random as suggested.

Employing the information described above we also analyzed the particle distribution within chromatophores in order to determine if this distribution was ranodm, aggregative, or uniform [17], indicative therefore, of some form of substructure. What we found was clear in that the distribution of the VPUs within the plane of the membrane is highly structured; when carefully analyzed we observed that each VPU was neighbored by six VPUs, similar but not identical to that observed for Rhodopseudomonas viridis [12]. For example, if we take chromatophores and fuse them with phospholipid vesicles, we observed the following: the density of particles decreases as the protein to lipid decreases (Fig. 3b–d). Analyses of these data reveal that such a distribution is basically random and lacks substructure. Furthermore, the particle diameter does not change upon dilution with lipid, suggesting considerable protein-protein interaction within the VPU, which is not subject to dissociation following particle dilution and therefore implying the absence of subunit exchange between VPUs.

Finally, additional measurements, presented in Table I, reveal that the percent area covered by particles in asynchronous cultures for high, medium, and low light grown cells is 36, 43, and 56, respectively, giving an average edge to edge distance between particles of 5.52–4.92–3.32 nm, respectively. In synchronous cultures the percent area covered is 39.2 to 53.0 for an average edge to edge distance between particles of 5.68 to 3.32 nm. In liposome fusions with chromatophores we range from 17% to 50% of the area being covered by particles for an average edge to edge distance of 15.0 to 4.2 nm. Since the VPUs in medium light grown cells can occupy over 50% of the membrane area and account for 50% of the protein, the implication is that protein virtually occupies the entire membrane [9].

By direct measurement we estimate that the number of VPUs per chromatophore in the average cell in an asynchronously growing culture at moderate light intensity

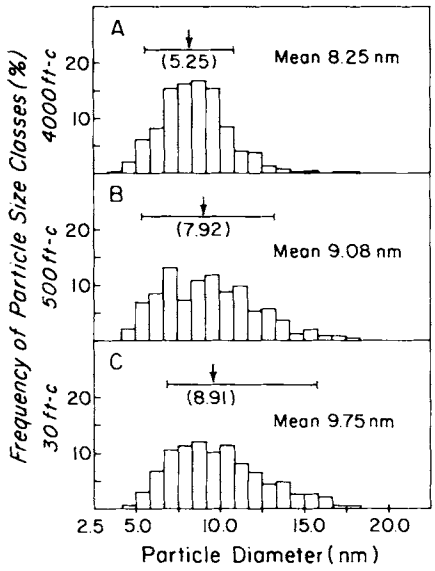

Fig. 6. Particle size histograms of intramembrane particles on the PF faces of chromatophores isolated from asynchronous cultures grown at 4000, 500, and 30 ft-c, respectively. Arrow indicates the mean particle size. Horizontal bar and number in parentheses indicate the range of particle size distribution in which 83.3% of the particle population measured are distributed around the mean. For the measurement of intramembrane particle size, electron micrographs were taken at 50,000×, enlarged to 150,000× and further optically enlarged to 1,200,000×. The diameter or long axis of the intramembrane particle was measured using a calibrated ruler. A total of 500–520 particles from several fracture faces were measured for each sample.

is approximately 50. Recently, we made a calculation of the number of VPUs per chromatophore based upon the protein and phospholipid composition and derived a value of 42 [10], in excellent agreement with the measured value.

We would interpret these results as suggesting that during the cell cycle new RC polypeptides together with the fixed antenna pigment protein complexes are inserted together into preexisting membrane, thereby increasing the particle density which is reflected in the observed changes in the protein to phospholipid ratio in chromatophores. Likewise, given the relative homogeneity in average particle size but the readily obvious threefold range in actual size distribution of these particles, at a given light intensity, but different for different light intensities, we would suggest that the variable antenna complex is inserted independently of the FPU and randomly associates with FPUs once in the membrane. Therefore, in the case of FPUs, new protein associates only with new protein, while in the case of the VPUs new protein in the form of B800-850 complexes may associate with either new or old protein. This particular form of regulation would be advantageous to the cell in that it would permit the ready adaptation of the cell to changes in light intensity.

Because we know that ICM phospholipid is transferred from outside the ICM to the ICM at the time of cell division [5] certain predictions derive from these observations: 1) Phospholipid biosynthetic activity should, by and large, reside outside the ICM. Such studies are currently underway in our laboratory and although

not yet completed it appears that phosphatidylglycerolphosphate synthetase and cytidylate transferase activities are located exclusively on the cytoplasmic membrane and virtually absent from the ICM. 2) There must exist a barrier restricting the free movement of phospholipid from the CM into the ICM, and that barrier must remain in place throughout most of the division cycle [1–5]. That the CM and ICM are continuous has been repeatedly demonstrated and need not be considered further here [6,7].

Because the phospholipids of the CM and ICM are identical in structure (as well as their relative proportions) we initially had to employ a kinetic approach in order to infer the localization of phospholipid biosynthetic activities and restricted movement of phospholipid species, between these membrane systems [1–5]. If we had a phospholipid species which was unique to a particular membrane system then these results would obtain additional support.

We have recently discovered and determined the structure of a new phospholipid species in R sphaeroides, namely N-acylphosphatidylserine (NAPS) [18]. Its structure is shown in Figure 7 and its unique position on two-dimensional thin layer plates is shown in Figure 8. Its discovery and structural determination were facilitated by the fact that certain strains of R sphaeroides, when grown in Tris containing minimal medium will accumulate this phospholipid to extremely high levels [19]. At approximately 20 mM Tris, the final cellular level of NAPS is approximately 30% of the total phospholipid of R sphaeroides strain 2.4.7 or its derivatives.

When present at these elevated levels, NAPS is found to be distributed equally in all of the cellular membrane fractions. As you will see shortly, NAPS is normally present in all R sphaeroides strains, but at very low levels.

We have previously shown that when employing a steady-state culture prelabeled with ^{32}P to saturate the P_i pools, the addition of Tris (20 mM final concentration) results in the instantaneous accumulation of label into NAPS [20]. There is both the immediate and sustained increase in the fraction of the phospholipid label in NAPS. Phosphatidylglycerol (PG) labeling remains unchanged while the fraction of the label incorporated into phosphatidylethanolamine (PE) undergoes an accelerated decline following Tris addition. Phosphatidylcholine (PC) shows a continuous slow increase, gradually leveling off to its steady-state concentration. This is due to the relatively slow movement of label through the large PE pool to PC in R sphaeroides.

However, when we contrast the behavior of accumulated NAPS to metabolic or normal levels of NAPS found in non-accumulating cells [19], ie, cells not exposed to Tris, NAPS is the phospholipid species together with PG which accumulate label the fastest [19], in accord with the presence of a NAPS and PG branch of phospholipid metabolism. As NAPS becomes an increasingly smaller fraction of the total cellular labeled phospholipid, the relative labeling of PE increases and PG labeling remains relatively constant. However, these results clearly show the very high metabolic activity of NAPS under conditions where this phospholipid species is non-accumulating.

Because of the very rapid turnover of metabolic NAPS we reasoned that this phospholipid may represent a unique phospholipid marker for the CM which might reveal its exclusion from the ICM over a short time frame inferring that its synthesis is largely restricted to the CM. Therefore, we followed the fraction of label in the various phospholipid species in a synchronously growing cell population following the introduction of ^{32}Pi at the time of cell division when we knew from previous

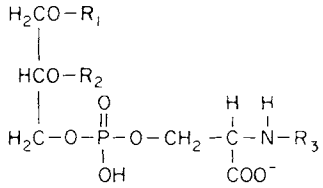

R_1, R_2, and R_3 represent fatty acid chains.

Average Fatty Acid Composition

85%	$C_{18:1}\Delta 11$	$R = \sim\overset{O}{\overset{\|\|}{C}}CH_2CH_2(CH_2)_6CH_2CH=CHCH_2(CH_2)_4CH_3$
9%	$C_{18:0}$	$R = \sim\overset{O}{\overset{\|\|}{C}}CH_2CH_2(CH_2)_{14}CH_3$
1%	$C_{16:1}\Delta 9$	$R = \sim\overset{O}{\overset{\|\|}{C}}CH_2CH_2(CH_2)_4CH_2CH=CHCH_2(CH_2)_4CH_3$
5%	$C_{16:0}$	$R = \sim\overset{O}{\overset{\|\|}{C}}CH_2CH_2(CH_2)_{12}CH_3$

Fig. 7. Structure of N-acylphosphatidylserine and fatty acid composition of bulk phospholipid [18].

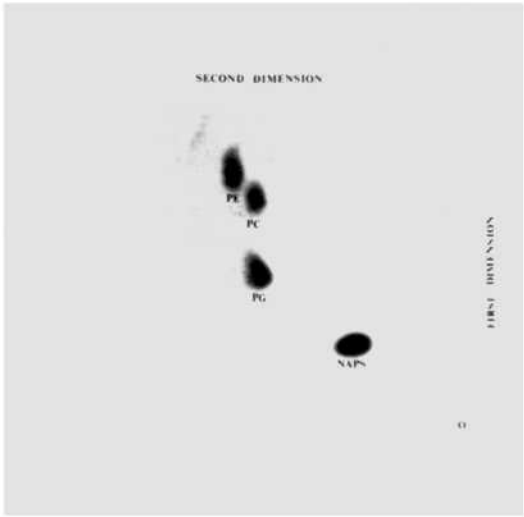

Fig. 8. Radioautogram of a two-dimensional thin layer chromatography separation of R sphaeroides phospholipids. Cells were grown in the presence of 20 mM Tris, and 10μ Ci/ml [^{32}P]-orthophosphoric acid for six culture doublings [18].

studies [5] that we can maximize the amount of phospholipid label being transferred to the ICM. The fraction of each phospholipid species was then determined for both whole cells and for isolated chromatophores. As can be seen in Figure 9, the fraction of label in NAPS in the chromatophores is only a small percentage of the total cellular label in NAPS, whereas the levels of label in PC and PG are very similar in both chromatophores and whole cells. The exclusion of metabolic NAPS from the ICM,

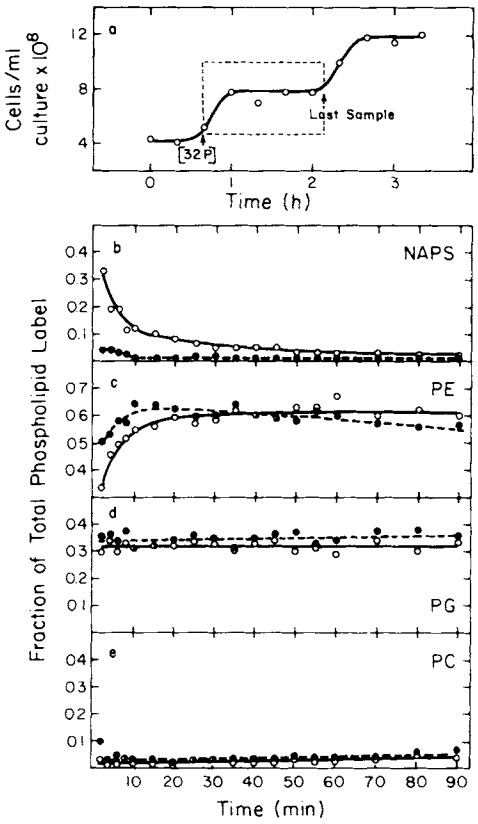

Fig. 9. Distribution of phospholipid label in cells and chromatophores in a synchronously dividing photoheterotrophic culture of R sphaeroides labeled with ^{32}Pi. ○, whole cells; ●, chromatophores [20].

over the time frame of the experiment, clearly demonstrates the restriction to free movement of phospholipid between these two functional domains of a continuous membrane system. To further demonstrate the validity of these results the identical experiment was performed with an asynchronously growing culture of R sphaeroides [20] and essentially identical results were obtained.

This very low level of NAPS label in the chromatophore fraction can be shown to result in part from contamination of the isolated chromatophores with CM fragments. Because of the large number of small samples being processed it is necessary to perform these experiments under conditions where the separation of ICM from CM (10–15% contamination) is not as clean as it could be (less than 5% contamination). We have previously shown that penicillin-binding protein (PBP) activity in phototrophically grown R sphaeroides resides exclusively within the CM [21]. Therefore, we determined the PBP content of our chromatophores when determining the presence of NAPS and were able to demonstrate that virtually all of the labeled NAPS could be accounted for by CM contamination of our chromatophores.

Therefore we conclude that: 1) Most newly synthesized NAPS resides within the CM and reveals the absence of free unimpeded phospholipid flow between the CM and ICM and 2) the residence of NAPS exclusively with the CM certainly suggests the CM is the virtually exclusive site of synthesis of this phospholipid species.

DISCUSSION

Let us consider our model of ICM replication under steady-state conditions as shown in Figure 1. Despite its continuity with the CM, it can remain structurally and functionally distinct with new protein being inserted into old membrane and phospholipid showing a cell-cycle specific dependency for its transfer into the ICM. The number of FPUs per unit of ICM oscillates as a function of the cell cycle. The phospholipids of the ICM remain relatively fixed, making the membrane semi-crystalline in nature at least through part of the division cycle. Proteins, such as some phospholipid biosynthetic enzymes and PBPs can be uniquely directed, either during or following their synthesis to the CM and not the ICM. Light-harvesting II polypeptides can, conversely, be directed to the ICM and not the CM. Some cytochromes, coupling factor, etc, can be directed to both membrane systems. Because new protein is directed to preexisting ICM invaginations we can only conclude that concommitant with the insertion of phospholipid into the ICM, these invaginations must themselves replicate prior to their partitioning to daughter cells.

Further, oxygen can regulate the presence or absence of the ICM and once present, it can serve to regulate the fate of residual ICM [21]. Light, on the other hand, can regulate both the amount of ICM per cell as well as the size of the VPU within the ICM. Finally, the cell cycle imposes additional controls on the VPU packing density, presumably independent of light intensity, as well as some form of intermembranous communication which signals the movement of cellular phospholipid, presumably between membrane systems.

To our knowledge these data represent the most comprehensive study of the biosynthesis of any membrane system but further, they describe a unique regulatory model during the cell cycle of the organism. This regulatory model for ICM replication in steady-state cells is in addition to those described for changes in light intensity [22] and anaerobiosis [22].

As these results presently stand, at least three very important questions are raised, namely: 1) What is the nature of the "barrier" restricting free lateral movement of phospholipid into the ICM; 2) what are the functional implications arising from the changing structural composition associated with the cell cycle; and 3) what physiologic parameters necessitate this mode of assembly?

As to the first question there are numerous possibilities involving specific protein or non-bilayer lipids, but no experimental evidence is yet available. As to the second question, studies are currently being conducted on chromatophores derived from synchronous cell populations, and so far it seems clear that a high protein to phospholipid composition results in a much more efficient electron transport chain and that chromatophores as routinely used only provide average values for such measurements. Last, although we have no evidence, it may be that cell division and the partitioning of the ICM to daughter cells requires a more fluid membrane system,

whereas functionally the system is more efficient at higher protein to lipid ratios. Therefore, the cell compromises these needs in the manner described here.

Finally, we must consider the findings summarized here with those observed for other experimental systems involving ICM biosynthesis. Direct comparisons are difficult to make for the following reasons: 1) Numerous studies have been performed with Rhodospirillum rubrum [23] and others with Rhodopseudomonas capsulata [24]; 2) many studies either involved the induction of ICM biogenesis following a switch from chemoheterotrophic to photoheterotrophic growth [24] or derepression of ICM synthesis following a shift-down in light intensity [25,26], and none involved the use of synchronous cell cultures. However, Niederman and colleagues have concluded [26] that growth of the ICM in R sphaeroides involves mainly the addition of new components to preexisting material and B800-850 complexes are not added to FPU until the latter are completely formed. Such conclusions are similar to those cited here. Niederman [26] has also documented the insertion of RC, LHI, and LHII into sites other than the ICM. However, such experiments were performed under conditions of ICM induction when new invaginations are being formed. Such conditions are not steady-state and cannot be extended to these studies.

The situation is somewhat more difficult to interpret in the case of R capsulata where ICM formation is never quite shut down [25], and when conditions favoring photoheterotrophic growth are restored, new as well as preexisting invaginations serve as the matrix for incorporation of new materials. Although the assembly process has been followed by Drews and his colleagues, direct comparisons between these results and those reported here are difficult since cells were either undergoing induction [24] or derepression [25] and steady-state systems were not investigated. In an earlier study, Golecki et al [27] concluded that cells of R capsulata grown at very low light intensities increased the amount of ICM per cell, as well as the size and number of VPUs relative to high light grown cells. These conclusions are similar to those reported here where we observe increased ICM per cell, increased size of the VPU, and increased (10%) VPUs per unit ICM.

Further, the recent results of Varga and Staehelin [13] clearly demonstrate an inverse relationship between light intensity and size of the VPU which is an important finding in the present studies. Although several studies [13,27] have measured the VPU particle size and number and have shown that the size distribution is basically normal, it is interesting that the smallest particle size measured is approximately 5 nm and the largest approximately 15–18 nm as shown here. However, because we were able to measure these size distributions as a function of the cell cycle we were able to conclude that distributions in particle sizes resulted from the random addition of B800-850 complexes to FPUs.

Finally, an inescapable conclusion of all of our data is that under steady-state conditions the number of invaginations per cell remains constant and is accomplished by the division of preexisting invaginations following the cell cycle specific insertion of phospholipid concurrent with cell division. It should be possible to follow this process employing an electronmicroscopic analysis of synchronous cell cultures employing techniques similar to those of Golecki and Oelze [23]. These investigators observed that there was no direct correlation between the number of invaginations per unit area of cytoplasmic membrane and the cellular Bchl content, which would support our results presented here. However, care must be taken in extending these data since the experiments of Golecki and Oelze were conducted with R rubrum

under conditions of ICM induction using asynchronous cultures grown to fairly high cell densities and therefore also undergoing derepression of ICM synthesis at later times.

This diversity of experimental systems and methodologies notwithstanding, it should be clear to anyone interested in membrane biosynthesis in general and photosynthetic membranes in particular that an accurate and detailed framework for photosynthetic membrane assembly in the photosynthetic bacteria is within reach.

ACKNOWLEDGMENTS

This work was supported by PHS grant GM15590 to SK. TJD was a recipient of a PHS postdoctoral fellowship 1-F32-GM07633-01.

REFERENCES

1. Lueking DR, Fraley RT, Kaplan S: J Biol Chem 253:451, 1978.
2. Fraley RT, Lueking DR, Kaplan S: J Biol Chem 253:458, 1978.
3. Wraight CA, Lueking DR, Fraley RT, Kaplan S: J Biol Chem 253:465, 1978.
4. Fraley RT, Lueking DR, Kaplan S: J Biol Chem 254:1980, 1979.
5. Cain BD, Deal CD, Fraley RT, Kaplan S: J Bacteriol 145:1154, 1981.
6. Reed DW, Raveed D: Biochim Biophys Acta 283:79, 1972.
7. Drews G, Oelze J: Adv Microbiol Physiol 22:1, 1981.
8. Fraley RT, Jameson DM, Kaplan S: Biochim Biophys Acta 511:52, 1978.
9. Fraley RT, Yen GSL, Lueking DR, Kaplan S: J Biol Chem 254:1987, 1979.
10. Kaplan S, Arntzen C: In Govindjee (ed): "Photosynthesis: Energy Conversion by Plants and Bacteria," vol 1, New York: Academic Press, 1982 pp 65–151.
11. Shiozawa JA, Welte W, Hodapp N, Drews G: Arch Biochem Biophys 213:473, 1982.
12. Miller KR: Nature 300:53, 1982.
13. Varga AR, Staehelin LA: J Bacteriol 154:1414, 1983.
14. Yen GSL, Wraight CA, Kaplan S: Biochim Biophys Acta 688:605, 1982.
15. Fraker PJ, Kaplan S: J Bacteriol 108:465, 1971.
16. Kosakowski MH, Kaplan S: J Bacteriol 118:1144, 1974.
17. deLaat SW, Tertoolen LGJ, Bluemink JG: Eur J Cell Biol 23:273, 1981.
18. Donohue TJ, Cain BD, Kaplan S: Biochemistry 21:2765, 1982.
19. Donohue TJ, Cain BD, Kaplan S: J Bacteriol 152:595, 1982.
20. Cain BD, Donohue TJ, Kaplan S: J Bacteriol 152:607, 1982.
21. Shepherd WD, Kaplan S, Park JT: J Bacteriol 147:354, 1981.
22. Kaplan S: In Clayton RK, Sistrom WR (eds): "The Photosynthetic Bacteria," New York: Plenum Press, 1978, pp 809–835.
23. Golecki JR, Oelze J: J Gen Microbiol 88:253, 1975.
24. Kaufman N, Reidl HH, Golecki JR, Garcia AF, Drews G: Arch Microbiol 131:313, 1982.
25. Dierstein R, Schumacher A, Drews G: Arch Microbiol 128:376, 1981.
26. Hunter GN, Pennoyer JD, Niederman RA: In: "Cell Function and Differentiation, Part B," New York: Alan R. Liss, 1982, pp 257–265.
27. Golecki JR, Schumacher A, Drews G: Eur J Cell Biol 23:1, 1980.